Postprint of: Kozieł S., Pietrenko-Dąbrowska A., Accelerated Gradient-Based Optimization of Antenna Structures Using Multi-Fidelity Simulations and Convergence-Based Model Management Scheme, IEEE TRANSACTIONS ON ANTENNAS AND PROPAGATION, (2021), pp. 1-12, DOI: 10.1109/TAP.2021.3083742

Accelerated Gradient-Based Optimization of Antenna Structures Using Multi-Fidelity Simulations and Convergence-Based Model Management Scheme

Slawomir Koziel, *Senior Member*, *IEEE*, and Anna Pietrenko-Dabrowska, *Senior Member*, *IEEE*

***Abstract*—The importance of numerical optimization has been steadily growing in the design of contemporary antenna structures. The primary reason is the increasing complexity of antenna topologies, [a typically large number of adjustable parameters that have to be simultaneously tuned. Design closure is no longer possible using traditional methods, including theoretical models or supervised parameter sweeping. To ensure reliability, optimization is normally carried out at the level of full-wave electromagnetic (EM) simulations, which incurs major computational expenses. The issue can be alleviated using a variety of methods such as the incorporation of adjoint sensitivities, sparse sensitivity updates (for local optimization), or the employment of surrogate modeling methods (in the context of global search). Another possibility is utilization of variable-fidelity simulation models, which, in practice, is most often restricted to two levels (coarse/fine or low-/high-fidelity models), and accompanied by appropriate low-fidelity model correction (e.g., space mapping). This paper proposes an accelerated version of a trust-region gradient-based procedure, which involves simulation model management by continuous adjustment of EM analysis fidelity throughout the optimization process. Decision making process is based on the convergence status of the algorithm. The initial stages of the optimization run are executed using the coarsest discretization of the structure at hand with the model being gradually refined towards the end of the process. This enables considerable computational savings without degrading the quality of the final design. The presented approach has been comprehensively validated using a benchmark set of four broadband antennas and compared to the reference trust-region procedure and two state-of-the-art accelerated algorithms. The average computational savings are almost sixty percent as compared to the reference.**

***Index Terms*— EM-driven optimization; multi-fidelity simulations; model management; decision making.**

I. Introduction

Performance requirements imposed on contemporary antenna systems are dictated by the needs of particular applications, and tend to be increasingly stringent, especially in the case of emerging areas such as the internet of things (IoT), wireless communication technologies (e.g., 5G [1]), medical imaging [2], or implantable devices [3]. The specifications are pertinent to both electrical (impedance matching) and field characteristics (gain, radiation pattern, efficiency), as well as various functionalities (multi-band operation, pattern diversity [4], circular polarization [5], etc.). Their fulfilment requires meticulous design, which is normally a multistep process involving conceptual development, topology evolution, as well as the final tuning of antenna dimensions [6]. Although parametric studies are still routinely carried out, especially at the initial design stages, their role is nowadays limited to demonstrate the importance of particular alterations incorporated into the antenna geometry [7]. On the other hand, numerical optimization has become instrumental in achieving adequate performance, especially when handling a large number of system variables, objectives, and constraints [8]. Unfortunately, in a vast majority of practical situations, the parameter tuning has to be realized at the level of full-wave electromagnetic (EM) simulation models [9], which might be a challenging endeavour. The major bottleneck are significant computational expenses entailed by massive system simulations required by numerical procedures [10], often prohibitive. These may be problematic even in the case of local tuning (e.g., gradient-based [11], [12], pattern search [13]), let alone global optimization (nature-inspired procedures [14]-[18]), or uncertainty quantification [19], including statistical analysis [20] and robust design [21].

In the light of the aforementioned issues, the development of computationally efficient techniques is a prerequisite for widespread utilization of numerical optimization in antenna design. The analysis of available literature reveals the two major groups of methods addressing high-cost of EM-driven design. The first consists of strictly algorithmic improvements, primary targeting acceleration of gradient-based procedures. These include incorporation of adjoint sensitivities [22], as well as sparse sensitivity updates (e.g., utilization of updating formulas [23]). The second group includes surrogate-assisted

The manuscript was submitted on December 28, 2020. This work was supported in part by the Icelandic Centre for Research (RANNIS) Grant 217771, and by National Science Centre of Poland Grant 2020/37/B/ST7/01448.

S. Koziel is with Engineering Optimization and Modeling Center of Reykjavik University, Reykjavik, Iceland (e-mail: koziel@ru.is); A. Pietrenko-Dabrowska and also S. Koziel are with Faculty of Electronics, Telecommunications and Informatics, Gdansk University of Technology, 80-233 Gdansk, Poland.

methods that rely on either physics-based [24] or data-driven surrogates [25]. Physics-based techniques capitalize on the problem-specific knowledge embedded in an underlying low-fidelity representation of the system at hand (coarse-discretization EM simulations [26], equivalent networks [27]) to yield a reliable model featuring good generalization capability. Some popular methods of this group include space mapping [28], adaptive response scaling [29], feature-based optimization [30], or cognition-driven design [31]. Data-driven surrogates (kriging [32], radial basis functions [33], Gaussian process regression [34], polynomial chaos expansion [35], neural networks [36], support vector regression [37]) are either used as overall replacements of expensive EM simulations [38], or, more often, in conjunction with sequential sampling techniques [39] to gradually build up (globally) accurate models using the data accumulated in the course of the optimization run [40], [41]. Notwithstanding, application of data-driven surrogates in high-frequency design is severely hindered by a typically strong nonlinearity of system responses (e.g., resonant characteristics of multi-band antennas [42]), but also the curse of dimensionality. Reported case studies normally feature just a few (up to six) independent parameters [43]-[45]. An alternative approach is utilization of a system-by-design [46]-[50], which comprehensively handles the design process, including synthesis, analysis, configuration and optimization under a single framework.

Recently, several methods belonging to the system-by-design approach to antenna design have been reported [46]-[50], which comprehensively handles the design process from system synthesis and analysis through configuration to optimization.

Despite the importance of global search procedures for specific application areas such as pattern synthesis in antenna array design [51], or radar cross section reduction using metasurfaces [52], majority of practical optimization scenarios are related to local parameter tuning. This is because reasonable initial designs are often obtained at the earlier stages of antenna development (e.g., in the course of topology evolution). As mentioned before, gradient-based procedures can be greatly accelerated using adjoint sensitivities, yet this technology is not widely available in commercial simulation packages. Variable-fidelity methods such as space mapping [24], or response correction techniques [53] can also be used to improve the computational efficiency but these methods require careful selection of the low-fidelity model and a particular correction technique [54]. Viable alternatives have been offered by sparse sensitivity updating schemes (e.g., based on the analysis of design relocation between algorithm iterations [55] or adaptive Broyden updates [56]), also combined with response feature technology [23]. These methods offer up to sixty percent speedup with only slight degradation of design quality as compared to the reference algorithms [55]-[56]. Additional benefits can be achieved by means of multi-fidelity simulation models; however, appropriate model management is not a trivial task [57].

This paper proposes a novel technique that incorporates EM simulations of varying resolution into the trust-region gradient search algorithm. The decision making process concerning the discretization level of the antenna structure under design is controlled by the convergence status of the optimization process as well as the objective function improvements obtained in subsequent algorithm iterations. Initiating the optimization run from the coarsest model allows for inexpensive exploitation of the knowledge about the system under design, as well as fast exploration of the parameter space. At the same time, increasing the model fidelity in the later stages ensures reliability of the design process. Our methodology is demonstrated through impedance matching optimization of several broadband antennas. To validate its efficacy, comprehensive comparisons with the reference trust-region algorithm as well as several accelerated routines are carried out. The average speedup obtained across the considered benchmark set is almost sixty percent over the reference, while ensuring better design quality than the accelerated procedures of [23] and [55].

The novelty and the technical contributions of this work include: (i) conceptual development of the convergence-based model fidelity management scheme enabling low-cost and reliable design optimization of antenna structures, (ii) implementation of the optimization algorithm integrating local gradient-based search with automated adjustment of the model discretization level, (iii) demonstrating a significant speedup of the search process that can be achieved by means of the introduced framework with only slight degradation of the design quality. The major difference between the approach proposed in this work and the previous attempts concerning multi-scale models is that the framework considered here allows for automated adjustment of model resolution based on convergence-related factors; this is done in a continuous manner and it is not restricted to a pre-defined set of two or three resolutions.

II. Accelerated Antenna Optimization by Multi-Fidelity Simulation Models and Convergence-Based Model Management

This section introduces the proposed optimization approach involving multi-fidelity EM simulations. The core algorithm is a conventional trust-region gradient-based procedure with numerical derivatives. Multi-fidelity simulations are incorporated by making the antenna discretization density dependent on the convergence status of the search process, starting from the lowest-fidelity representation, and gradually increased towards the end of the algorithm run. This allows for accelerating the initial stages of parameter space exploration by exploiting the problem-specific knowledge encoded in the low resolution models, while maintaining the reliability. The section starts by formulating the antenna parameter adjustment task (Section II.*A*), and recalling the conventional trust-region algorithm (Section II.*B*). Section II.*C* discusses multi-fidelity models, whereas the proposed optimization procedure is outlined in Sections II.*D* and II.*E*.

A. Simulation-Based Antenna Optimization

Numerical optimization has been playing a more and more important role in the design of modern antenna structures,

especially, in the last part of the development process where the antenna topology is already established, yet geometry parameters need to be tuned to ensure the best attainable performance [25]. This process is often referred to as design closure and requires a definition of an appropriate metric that allows us to quantify the design quality. In practice, one often needs to account for multiple objectives (e.g., simultaneous improvement of in-band matching and gain); however, multi-objective optimization (e.g., [58]) is not considered in this work. Handling several objectives through single-objective optimization can be arranged by aggregation (e.g., weighted sum method [59]) or by selecting a primary objective while handling the remaining ones by means of constraints with pre-defined acceptance thresholds. Although the former approach is conceptually straightforward, it does not ensure sufficient control over the design goals. Consequently, in this work, the design closure task is formulated according to the latter paradigm. We denote as $\boldsymbol{x}$ the vector of adjustable parameters of the antenna of interest. The optimum design is found by solving

$$\boldsymbol{x}^* = \arg\min_{\boldsymbol{x}} U(\boldsymbol{x}) \tag{1}$$

subject to $g_k(\boldsymbol{x}) \le 0$, $k = 1, \ldots, n_g$, and $h_k(\boldsymbol{x}) = 0$, $k = 1, \ldots, n_h$ (inequality and equality constraints, respectively). The objective function U is defined to reflect the designer's understanding of the antenna performance so that better designs correspond to lower values of $U(\boldsymbol{x})$. For the sake of clarity, let us consider some examples:

- Design for best in-band matching: $U(\boldsymbol{x}) = S(\boldsymbol{x}) = \max\{f \in F : |S_{11}(\boldsymbol{x},f)|\}$, where f is a frequency within intended operating range F of the antenna;
- Design for maximum gain: $U(\boldsymbol{x}) = -G(\boldsymbol{x})$, where $G(\boldsymbol{x})$ is the average or maximum in-band gain. Typically, the constraint $S(\boldsymbol{x}) \le -10$ dB is imposed in order to ensure sufficient impedance matching of the structure;
- Design for axial ratio improvement: $U(\boldsymbol{x}) = A_R(\boldsymbol{x})$, where $A_R(\boldsymbol{x}) = \max\{f \in F : AR(\boldsymbol{x},f)\}$ is the maximum in-band axial ratio. Similarly as before, the constraint $S(\boldsymbol{x}) \le -10$ dB is imposed to enforce appropriate impedance bandwidth;
- Design for size reduction of a circularly polarized antenna: $U(\boldsymbol{x}) = A(\boldsymbol{x})$, where $A(\boldsymbol{x})$ is the footprint; constraints $S(\boldsymbol{x}) \le -10$ dB, and $A_R(\boldsymbol{x}) \le 3$ dB.

One needs to emphasize that the evaluation of constraints related to electrical or field properties of the antenna requires EM simulation, therefore, their explicit handling is problematic. Instead, a penalty function approach is preferred [60], which leads to the following formulation of the design closure task:

$$\boldsymbol{x}^* = \arg\min_{\boldsymbol{x}} U_P(\boldsymbol{x}) \tag{2}$$

where the objective function U_P is a compound of the function U and the penalty terms of the form

$$U_P(\boldsymbol{x}) = U(\boldsymbol{x}) + \sum_{k=1}^{n_g+n_h} \beta_k c_k(\boldsymbol{x}) \tag{3}$$

In (3), $c_k(\boldsymbol{x})$ quantify violations of the respective constraints, whereas β_k are the penalty coefficients. An example of a penalty function, here, pertinent to the constraint $S(\boldsymbol{x}) \le -10$ dB, would be $c(\boldsymbol{x}) = [(S(\boldsymbol{x}) + 10)/10]^2$. Using the second power ensures smoothness of U_P at boundary of the feasible region, which is important from the numerical perspective because most constraints are active at the optimum. Furthermore, the power factor can be used to control the stiffness of the constraint, with the second power enabling tolerance for small violations.

B. Gradient-Based Optimization Using Trust Regions

The multi-fidelity optimization procedure proposed in this work is based on the conventional trust-region (TR) gradient-based algorithm [61], briefly outlined below. The same algorithm is also used as one of the benchmark methods. The TR algorithm solves the problem (2) in an iterative manner, where in the ith iteration, a new approximation $\boldsymbol{x}^{(i+1)}$ of the optimum solution $\boldsymbol{x}^*$ is rendered through constrained optimization of the local model $U_L^{(i)}$. The latter is most often based on the first-order Taylor expansion of relevant antenna characteristics, established at the current iteration point $\boldsymbol{x}^{(i)}$. In the case of reflection response, we would have

$$S_L^{(i)}(\boldsymbol{x},f) = S_{11}(\boldsymbol{x}^{(i)},f) + \boldsymbol{G}_S(\boldsymbol{x}^{(i)},f)\cdot(\boldsymbol{x}-\boldsymbol{x}^{(i)}) \tag{4}$$

where $\boldsymbol{G}_S(\boldsymbol{x}^{(i)},f)$ represents the gradient of S_{11} at $\boldsymbol{x}^{(i)}$ and frequency f. $U_L^{(i)}$ is defined the same way as U_P but with $S_L^{(i)}(\boldsymbol{x})$ replacing S_{11} (similarly for other types of responses, e.g., gain, axial ratio, etc.).

The optimization sub-problem is then formulated as

$$\boldsymbol{x}^{(i+1)} = \arg\min_{\boldsymbol{x};\, -\boldsymbol{d}^{(i)} \le \boldsymbol{x}-\boldsymbol{x}^{(i)} \le \boldsymbol{d}^{(i)}} U_L^{(i)}(\boldsymbol{x}) \tag{5}$$

In the reference algorithm, the antenna sensitivities are estimated using finite differentiation, which incurs additional n EM evaluations of the structure at hand per iteration (n being the parameter space dimensionality). The trust region is an interval $[\boldsymbol{x}^{(i)} - \boldsymbol{d}^{(i)}, \boldsymbol{x}^{(i)} + \boldsymbol{d}^{(i)}]$, which allows us to account for different ranges for various parameters and avoid variable scaling by making the initial size vector $\boldsymbol{d}^{(0)}$ proportional to the parameter space bounds [55]. The design $\boldsymbol{x}^{(i+1)}$ is accepted if it leads to the improvement of the objective function, i.e., $U_P(\boldsymbol{x}^{(i+1)}) < U_P(\boldsymbol{x}^{(i)})$. Otherwise, the TR size vector $\boldsymbol{d}^{(i)}$ is reduced [55], and the iteration is repeated.

Several accelerated versions of the algorithm (5) have been recently proposed, where full finite differentiation is replaced by sparse sensitivity updates using various mechanism such as design relocation tracking [55] or gradient variability tracking [56]. Some of these methods will be used as benchmark techniques in Section III of this work.

C. Multi-Fidelity Simulation Models

The main acceleration mechanism employed in this paper is the incorporation of multi-fidelity EM simulations. As mentioned in the introduction, variable-fidelity methods have been gaining popularity over the last two decades or so; however, these methods typically use two levels of models, referred to as coarse (low-fidelity), and fine (high-fidelity), with the coarse model often based on equivalent networks (microwave engineering [27]), or coarse discretization EM analysis (antenna design [26]). The coarse model typically undergoes an appropriate correction, and becomes a prediction tool that replaces the high-fidelity model in the search process. Some of popular methods of this sort include space mapping [24], manifold mapping [62], as well as response correction techniques [28]. Lower fidelity models can be also used for initial space exploration within machine learning frameworks

[63], or variable-fidelity modelling methods (e.g., co-kriging [64]). In general, appropriate selection of the low-fidelity model is a non-trivial task as it affects both the reliability of the optimization process and its computational efficiency [54].

Figure 1 shows two examples of antenna structures along with a family of reflection responses evaluated at different levels of structure discretization, here, parameterized using LPW (lines per wavelength), utilized in CST Microwave Studio to control the mesh density. Note that the simulation times are considerably longer for the monopole antenna, which is due to the SMA connector incorporated into the computational model. Clearly, using coarser discretization makes the simulation faster but at the expense of quality degradation. At certain levels of mesh densities, the model is no longer usable because the deviations from the high-fidelity representation are too large.

Based on visual inspection of antenna responses, one can establish the lowest LPW that is of practical utility (denoted as $L_{\min}$), and the LPW corresponding to the high-fidelity model that ensures sufficient accuracy in terms of representing the system characteristics (denoted as $L_{\max}$). In this paper, the aim is to accelerate the optimization algorithm by using the models within the range $L_{\min} \le L \le L_{\max}$ so that the reduced evaluation time of coarse-discretization simulations is translated into the improved computational efficiency of the search process. Section II.*D* describes the main prerequisites assumed to develop the strategy for adjusting the model fidelity along with the specific discretization density adaptation scheme.

D. Convergence-Based Model Management

The primary goal of the model management procedure is to control the EM model fidelity level in the course of the optimization process. The optimization engine of choice in this work is the TR algorithm outlined in Section II.*B*. As mentioned in Section II.*C*, we assume that the model fidelity is controlled using a single parameter L within a range L_{min} (lowest usable discretization density) to L_{max} (high-fidelity antenna representation). The development of the decision making scheme is based on the following prerequisites:

- The initial stages of the optimization process should be executed using the lowest-fidelity model to facilitate a reduction of the computational cost of the algorithm, thus allowing for exploitation of the knowledge about the system under design at a low cost;
- The final stages of the optimization process should be based on the high-fidelity model to ensure reliability;
- The transition between the models of various fidelities, should be based on the convergence status of the algorithm, in particular $\|\boldsymbol{x}^{(i+1)} - \boldsymbol{x}^{(i)}\|$ (convergence in argument), as well as the improvement of the objective function value $U_P(\boldsymbol{x}^{(i+1)}) - U_P(\boldsymbol{x}^{(i)})$;
- The transition should be possibly smooth with respect to the aforementioned criteria in order to maintain stability of the optimization process.

We also use some additional parameters, in particular, the termination thresholds ε_x and ε_U. Using these, the algorithm is terminated if either of the conditions is satisfied: $\|\boldsymbol{x}^{(i+1)} - \boldsymbol{x}^{(i)}\| < \varepsilon_x$, $\|\boldsymbol{d}^{(i)}\| < \varepsilon_x$, or $|U_P(\boldsymbol{x}^{(i+1)}) - U_P(\boldsymbol{x}^{(i)})| < \varepsilon_U$. In our numerical experiments we use $\varepsilon_x = 10^{-3}$, and $\varepsilon_U = 10^{-3}$. Let us define an auxiliary variable

$$Q^{(i)}(\varepsilon_x, \varepsilon_U) = \max\left\{\frac{\varepsilon_x}{\|\boldsymbol{x}^{(i+1)} - \boldsymbol{x}^{(i)}\|}, \frac{\varepsilon_U}{|U_P(\boldsymbol{x}^{(i+1)}) - U_P(\boldsymbol{x}^{(i)})|}\right\} \quad (6)$$

The specific management scheme developed in this work modifies the discretization parameter $L^{(i)}$ at the iteration i of the optimization algorithm as follows:

$$L^{(i+1)} = \begin{cases} L_{\min} & \text{if } Q^{(i)}(\varepsilon_x, \varepsilon_U) \le M \\ \max\left\{L^{(i)}, L_{\min} + (L_{\max} - L_{\min})\left[Q^{(i)}(\varepsilon_x, \varepsilon_U) - M\right]^{\frac{1}{\alpha}}\right\} \end{cases} \quad (7)$$

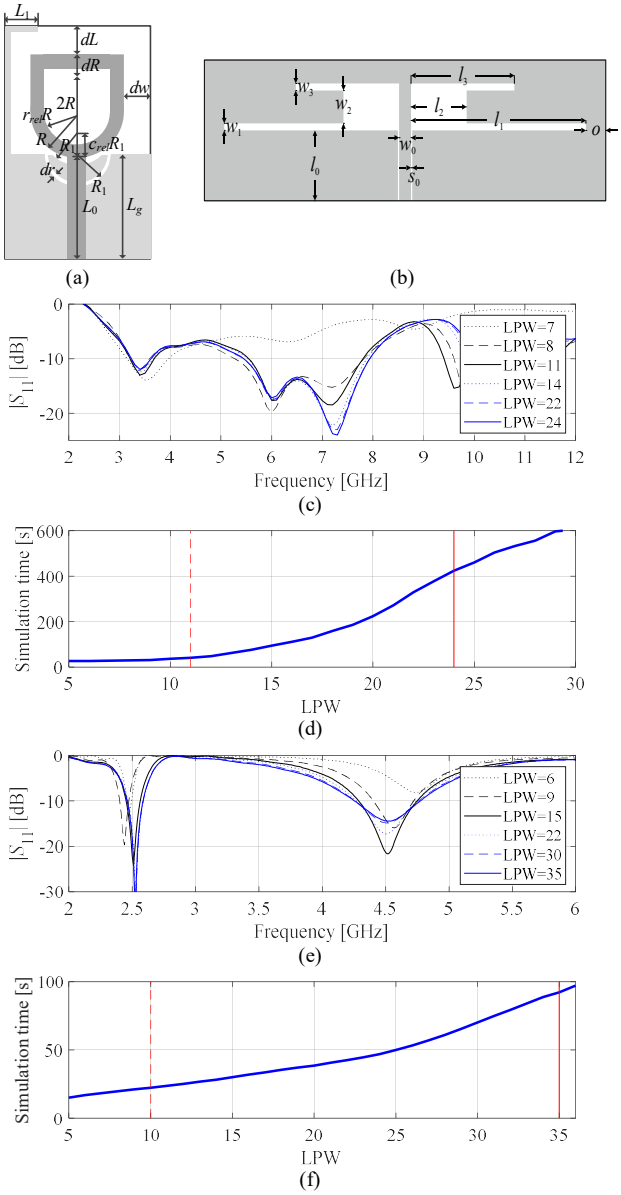

Fig. 1. Multi-fidelity simulation models for: (a) a broadband monopole antenna, and (b) a dual-band dipole antenna. Shown are: (a), (b) the antenna structures, (c), (d) the family of reflection responses corresponding to various discretization densities of the structure (controlled using the LPW parameter) (for the antenna of Fig. 1(a) and 1(b), respectively), as well as (e), (f) the relationship between LPW and simulation time (averaged over several antenna geometries) (also for the antenna of Fig. 1(a) and 1(b), respectively). The vertical lines denote the mesh density corresponding to the high-fidelity model (—) and the lowest usable low-fidelity one (- - -).

This article has been accepted for publication in a future issue of this journal, but has not been fully edited. Content may change prior to final publication. Citation information: DOI 10.1109/TAP.2021.3083742, IEEE Transactions on Antennas and Propagation

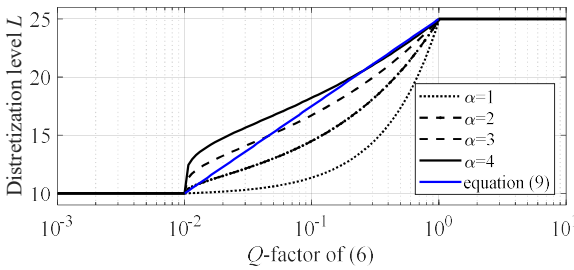

Fig. 2. Discretization level profiles obtained using equation (7) for various values of the control parameter α, as well as a piece-wise profile produced by equation (9). For the sake of illustration, the plots were created for $L_{min} = 10$, $L_{max} = 25$, and $M = 10^{-2}$.

1. Set the iteration counter $i = 0$, and $L^{(i)} = L_{min}$;
2. Evaluate antenna response $\boldsymbol{R}(\boldsymbol{x}^{(i)})$ at the discretization level $L^{(i)}$;
3. Evaluate antenna sensitivities $\boldsymbol{J}_R(\boldsymbol{x}^{(i)})$ at the discretization level L_{FD} (cf. (10));
4. Construct a linear model
   $\boldsymbol{L}^{(i)}(\boldsymbol{x}) = \boldsymbol{R}(\boldsymbol{x}^{(i)}) + \boldsymbol{J}_R(\boldsymbol{x}^{(i)}) \cdot (\boldsymbol{x} - \boldsymbol{x}^{(i)})$;
5. Obtain the design $\boldsymbol{x}^{(i+1)}$ by solving (5);
6. Evaluate antenna response $\boldsymbol{R}(\boldsymbol{x}^{(i+1)})$ at the discretization level $L^{(i)}$;
7. Update trust-region size vector $\boldsymbol{d}^{(i)}$ [55];
8. **if** $U_P(\boldsymbol{x}^{(i+1)}) < U_P(\boldsymbol{x}^{(i)})$
   Compute $L^{(i+1)}$ using (7);
   Set $i = i + 1$;
   end
9. **if** $\|\boldsymbol{x}^{(i+1)} - \boldsymbol{x}^{(i)}\| < \varepsilon_x$ OR $\|\boldsymbol{d}^{(i)}\| < \varepsilon_x$ OR $|U_P(\boldsymbol{x}^{(i+1)}) - U_P(\boldsymbol{x}^{(i)})| < \varepsilon_U$
   if $L^{(i)} < L_{max}$
   Set $L^{(i)} = L_{max}$ and modify $\boldsymbol{d}(i)$ according to (8);
   go to 3;
   else
   Go to 10;
   end
   else
   Go to 3;
   end
10. END.

Fig. 3. Operation of the proposed multi-fidelity optimization algorithm using the convergence-based decision making scheme. Here, all relevant EM-simulated antenna responses are collectively denoted as $\boldsymbol{R}(\boldsymbol{x})$, whereas $\boldsymbol{J}_R(\boldsymbol{x})$ denotes the sensitivity matrix, both at the design $\boldsymbol{x}$.

Note that the scheme is implemented to ensure monotonicity of the discretization parameters.

In Section III, we use $M = 10^{-2}$ and $\alpha = 3$. This makes the parameter L start to increase when the convergence indicators are two decades away from the algorithm convergence and the initial increase is relatively quick. The latter is reasonable due to the relationship between L and the simulation time; in particular, fast initial growth of L leads to accuracy improvements without entailing considerable computational overhead.

It should also be noted that formula (7) does not guarantee $L^{(i+1)}$ to ever reach L_{max} (e.g., when one or more iterations are unsuccessful and the algorithm terminates due to reduction of the TR size vector $\boldsymbol{d}^{(i)}$ beyond the termination condition). In order to ensure that the last stages of the optimization process are always carried out using the high-fidelity model, an additional mechanism is introduced. Upon termination of the algorithm, we set

$$\text{IF } L^{(i)} < L_{max} \text{ THEN } L^{(i+1)} = L_{max} \text{ AND } \boldsymbol{d}^{(i+1)} = \frac{M_d \boldsymbol{d}^{(i)} \varepsilon_x}{\|\boldsymbol{d}^{(i)}\|} \quad (8)$$

where the multiplication factor $M_d = 10$ in the numerical experiments of Section III. The operation (8) allows for bypassing the termination condition and executing further iterations with the discretization parameter set to L_{max}. Notwithstanding, this only happens if the value of this parameter was below L_{max} during the normal run of the algorithm.

Figure 2 shows the discretization level profile for several values of the control parameter α, as well as the profile corresponding to an alternative parameter-less equation

$$L^{(i+1)} = \begin{cases} L_{min} & \text{if } Q^{(i)}(\varepsilon_x, \varepsilon_U) \le M \\ \max\left\{L^{(i)}, L_{min} + (L_{max} - L_{min})\left[1 - \dfrac{\log(Q^{(i)}(\varepsilon_x, \varepsilon_U))}{\log M}\right]\right\} & \end{cases} \quad (9)$$

which results in a piece-wise linear transition between L_{min} and L_{max}. Note that $\alpha = 3$ gives the best approximation of (9) while allowing for more flexibility.

As an additional acceleration factor, when operating with the discretization level $L^{(i)}$, the antenna response sensitivities are evaluated using finite differentiation at lower fidelity level

$$L_{FD} = \max\left\{L_{min}, \lambda L^{(i)}\right\} \quad (10)$$

where $0 \le \lambda \le 1$ is another control parameter of the algorithm (in our numerical experiments, we use $\lambda = 2/3$). The rationale behind this approach is that although models of different fidelities are misaligned, they are typically well correlated (and the correlation is improving with the increasing values of $L^{(i)}$), which is sufficient to render reliable representation of the system response gradients.

E. Proposed Optimization Algorithm

The optimization algorithm proposed in this work is a combination of the trust-region procedure of Section II.*B*, and the multi-fidelity model management scheme of Section II.*D*. Its control parameters are:

- ε_x, ε_U – termination thresholds (cf. Section II.*D*);
- M – threshold for initiating discretization level increase (cf. Section II.*D*);
- α – discretization level shape parameter (cf. Section II.*D*);
- λ – control parameter for setting discretization level L_{FD} for finite differentiation (antenna sensitivity estimation), cf. (10);
- M_d – multiplication factor for increasing TR size in (8) (when closer to convergence).

The termination thresholds are decided by the user depending on the level of resolution that is required by the optimization process. The default values for other parameters are as discussed before: $M = 10^{-2}$, $\alpha = 3$, $\lambda = 2/3$, and $M_d = 10$. Furthermore, the minimum and maximum discretization level parameters L_{min} and L_{max} (cf. Section II.*C*) are decided upon by the user based on grid convergence study: L_{max} is the high-fidelity model (with the discretization level that ensures sufficient accuracy), and L_{min} is the lowest usable discretization that still ensures a proper rendition of all relevant details of the antenna characteristics. It can be noted that the algorithm only

contains four control parameters (except from the termination thresholds that are set up by the user depending on the required resolution of the optimization process). Among these, the initial experiments indicated that the algorithm performance is almost insensitive to the shape parameter α. Furthermore, the parameter λ can be precisely adjusted by through grid convergence studies concerning the accuracy of the low-fidelity sensitivity estimation as compared to the high-fidelity one; 2/3 is a value that is suitable for a typical microstrip antenna structure. The parameter M indicates the initiation of the discretization level increase has to be set to allow sufficient room for resolution manipulation, and two decades prior to convergence seem to be a good overall choice; also, it is not critical for the algorithm performance. The same can be said about the parameter M_d, which is rarely used anyway because, in most cases, the final discretization does reach L_{max}, in which case (8) is not executed. Clearly, for a particular optimization task, the optimum setup of control parameters may be different from the one provided here, but a common-sense adjustment as described above seem to work fine in most practical cases.

The operation of the algorithm can be summarized as shown in Fig. 3, where all EM-simulated antenna responses of interest are collectively denoted as $\boldsymbol{R}(\boldsymbol{x})$, whereas $\boldsymbol{J}_R(\boldsymbol{x})$ denotes the sensitivity matrix, both at the design $\boldsymbol{x}$; $\boldsymbol{x}^{(0)}$ stands for the initial design. Figure 4 shows the flow diagram of the algorithm. The matrix $\boldsymbol{J}_R(\boldsymbol{x})$ is estimated using finite differentiation. Assuming that $\boldsymbol{R}(\boldsymbol{x}) = [R(\boldsymbol{x},f_1)\ R(\boldsymbol{x},f_2)\ \ldots\ R(\boldsymbol{x},f_m)]^T$, where f_1 through f_m represent a discrete frequency sweep, and $\boldsymbol{x} = [x_1\ \ldots\ x_n]^T$, then $\boldsymbol{J}_R(\boldsymbol{x}) = [J_{ij}]_{i=1,\ldots,m;\ j=1,\ldots,n}$, where $J_{ij} = \partial R(\boldsymbol{x},f_i)/\partial x_j$, estimated as $J_{ij} \approx [R(\boldsymbol{x} + \boldsymbol{h}_i,f_j) - R(\boldsymbol{x} + \boldsymbol{h}_i,f_j)]/h$, where $\boldsymbol{h}_i = [0\ \ldots\ 0\ h\ 0\ \ldots\ 0]^T$ with 1 on the ith position, and h being the finite differentiation step.

Given a generic formulation of the optimization problem as well as the algorithm itself, it can be observed that the proposed framework can be applied to a variety of simulation-based design problems, not only antenna-related task. The only prerequisite is an availability of one (or more) control parameters that can be used to adjust the resolution of the computational model in a continuous manner.

III. Demonstration Case Studies and Benchmarking

This section provides numerical verification of the multi-fidelity algorithm introduced in Section II. Our studies are based on a benchmark set of four broadband antenna structures, optimized for best in-band matching. The results are compared to the standard trust-region gradient search procedure (cf. Section II.*B*), as well as two accelerated algorithms involving sparse sensitivity updates [23], [55]. All benchmark methods are briefly characterised in Section III.*B*. The main focus is on the computational cost of the optimization process as well as its reliability, i.e., the quality of the final designs rendered by the respective algorithms. The experimental validation of the designs of the presented benchmark antennas has not been provided as being irrelevant to the topic of the paper. Furthermore, all of the considered structures have been already validated not only in the respective source papers [65]-[68], but also in the papers regarding their numerical optimization (e.g., [23], [55]). Thus, the results provided in the remainder of this section suffice to substantiate the inferred conclusions, especially given the scope of this work, which, again, is the development of a novel optimization framework.

A. Benchmark Antenna Structures

The numerical experiments are carried out using four broadband antenna structures shown in Fig. 5. The relevant details have been gathered in Table I. The EM-simulation models are implemented in CST Microwave Studio and evaluated using the time-domain solver. All models incorporate the SMA connectors. The antennas are supposed to operate in UWB frequency range (3.1 GHz to 10.6 GHz), and are optimized to minimize the maximum in-band reflection within the operating band. Thus, the objective function is defined as $U(\boldsymbol{x}) = \max\{3.1\ \text{GHz} \le f \le 10.6\ \text{GHz} : |S_{11}(\boldsymbol{x},f)|\}$.

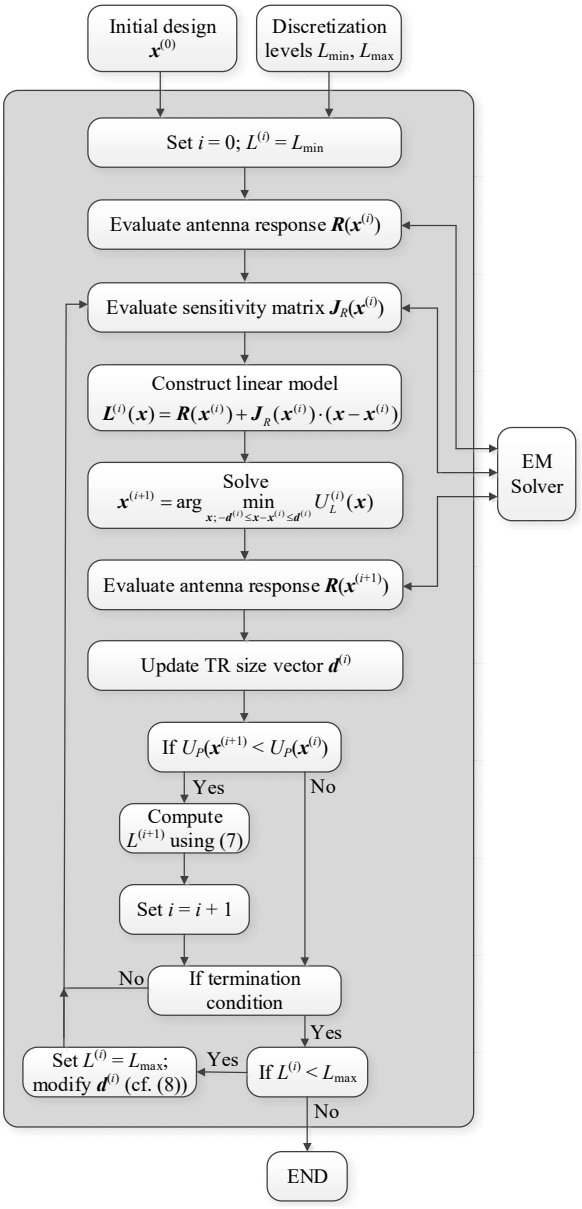

Fig. 4. Flow diagram of the proposed multi-fidelity optimization algorithm using the convergence-based decision making scheme.

This article has been accepted for publication in a future issue of this journal, but has not been fully edited. Content may change prior to final publication. Citation information: DOI 10.1109/TAP.2021.3083742, IEEE Transactions on Antennas and Propagation

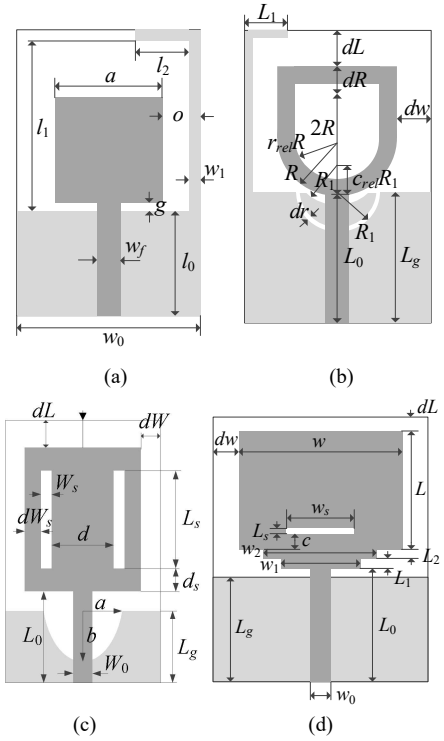

Fig. 5. Benchmark antenna structures: (a) Antenna I, (b) Antenna II, (c) Antenna III, (d) Antenna IV. Ground plane marked using light gray shade.

TABLE I BENCHMARK ANTENNA STRUCTURES

Antenna	Substrate	Designable Parameters [mm]	Other Parameters [mm]
I [65]	RF-35 (ε_r = 3.5, h = 0.762 mm)	$\boldsymbol{x} = [l_0\ g\ a\ l_1\ l_2\ w_1\ o]^T$	$w_0 = 2o + a$, $w_f = 1.7$
II [66]	RF-35 (ε_r = 3.5, h = 0.762 mm)	$\boldsymbol{x} = [L_0\ dR\ R\ r_{rel}\ dL\ dw\ Lg\ L_1\ R_1\ dr\ c_{rel}]^T$	$w_0 = 1.7$
III [67]	FR4 (ε_r = 4.3, h = 1.55 mm)	$\boldsymbol{x} = [L_g\ L_0\ L_s\ W_s\ d\ dL\ d_s\ dW_s\ dW\ a\ b]^T$	$W_0 = 3.0$
IV [68]	RO4350 (ε_r = 3.48, h = 0.762 mm)	$\boldsymbol{x} = [L_0\ L_1\ L_2\ L\ dL\ L_g\ w_1\ w_2\ w\ dw\ L_s\ w_s\ c]^T$	$w_0 = 1.7$

TABLE II STRUCTURE DISCRETIZATION DENSITY RANGE FOR ANTENNAS OF FIG. 5

Antenna	Lowest-fidelity model		High-fidelity model	
	L_{min}	Simulation time [s]	L_{max}	Simulation time [s]
I	10	42	21	150
II	11	41	24	424
III	10	46	20	265
IV	10	37	25	97

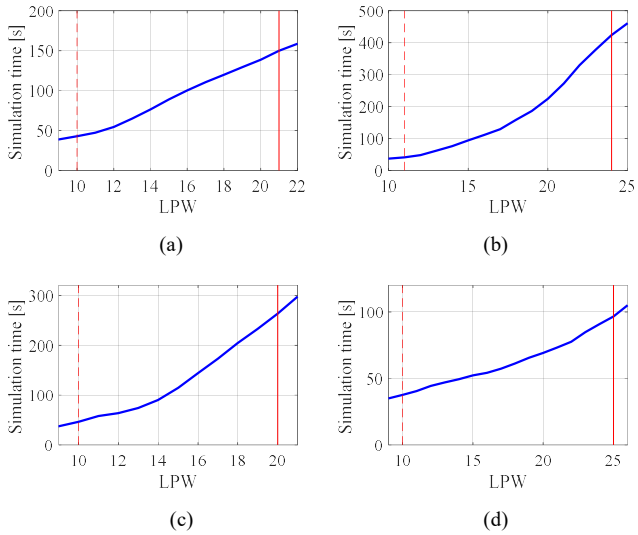

Fig. 6. Simulation time versus fidelity level for antennas of Fig. 5: (a) Antenna I, (b) Antenna II, (c) Antenna III, (d) Antenna IV. Vertical lines denote the LPWs corresponding to the minimum (- - -) and the maximum (—) considered level of fidelity for a given structure.

It can be observed that the time evaluation ratio between the high-fidelity model and the lowest-fidelity one varies between the structures from less than three for Antenna IV to around ten for Antenna II, with the average being slightly less than six. This suggests that the computational savings due to the incorporation of multi-fidelity modeling may be considerable. The critical factor here is exploitation of the problem-specific knowledge embedded in the lower-fidelity models, which can be acquired at a lot computational expenses.

B. Experimental Setup. Reference Algorithms

The numerical verification has been carried out in a statistical sense, based on ten independent algorithm runs executed from random initial designs. This setup is employed because the considered optimization problems are generally multimodal, whereas the optimization algorithms—both the proposed one and the benchmark—are the local routines. Due to that, initiating the search process from different starting points normally leads to different local optima. These are typically satisfactory from the point of view of antenna designer, yet distinct. One of the reasons for multimodality is that the considered antennas are compact structures with the geometries modified in order to facilitate size reduction. A byproduct is parameter redundancy that makes the functional landscape under optimization much more complex than it is for conventional radiators (in particular, monopoles).

Having this in mind, our goal is to estimate and compare the average performance of the algorithms. There are three criteria: (i) computational cost, (ii) design quality measured as the average objective function value, and (iii) repeatability of results (measured using standard deviation of the objective function values across the performed optimization runs). It should also be noted that given the aforementioned multimodality, it is expected that the standard deviation will be larger than zero even for the reference algorithm, i.e.,

This article has been accepted for publication in a future issue of this journal, but has not been fully edited. Content may change prior to final publication. Citation information: DOI 10.1109/TAP.2021.3083742, IEEE Transactions on Antennas and Propagation

conventional TR procedure based on high-fidelity simulations, which is presumably the most reliable among the compared methods. Consequently, potential repeatability degradation as measured by the standard deviation should be compared to that of the reference algorithm rather than to the zero value.

For the algorithm proposed in this work, the values of its control parameters were set as follows: $M = 10^{-2}$ (threshold for initiating discretization level increase; cf. Section II.*D*), $\alpha = 3$ (discretization level profile control parameter; cf. Section II.*D*), $\lambda = 2/3$ (control parameter for setting discretization level L_{FD} for finite differentiation; cf. (10), $M_d = 10$ (multiplication factor for increasing TR size in (8)). The termination thresholds $\varepsilon_x = \varepsilon_U = 10^{-3}$ (cf. Section II.*D*) are the same for all algorithms, the proposed one, and the benchmark.

There are three benchmark algorithms utilized for the sake of comparison:

- Algorithm 1: the reference TR algorithm as described in Section II.*D* exclusively using high-fidelity EM simulations (i.e., at the discretization level of $L_{\max}$ for the respective structures);
- Algorithm 2: the expedited version of the reference algorithm using solely high-fidelity EM simulations [55]. The main acceleration mechanism is to suppress some of the finite-differentiation (FD)-based Jacobian updates, based upon the magnitude of the relative design change with respect to the current TR region size. The design change between consecutive iterations is assessed by the selection factors defined as follows

$$\varphi_k^i = \left| x_k^{(i+1)} - x_k^{(i)} \right| \Big/ d_k^{(i)}, \quad k = 1, \ldots, n, \qquad (11)$$

where $x_k^{(i)}$, $x_k^{(i+1)}$ stand for the kth elements of the parameter vectors $\boldsymbol{x}^{(i)}$, $\boldsymbol{x}^{(i+1)}$ of the two most recent iterations, respectively, and $d_k^{(i)}$ refers to the kth entry of the TR region size vector $\boldsymbol{d}^{(i)}$. For a given parameter k, if φ_k^i is lower than a user-specified threshold, FD is not performed, and the previous value of the appropriate Jacobian column is retained. In order to enforce the update once in few iterations, the optimization history is inspected. The maximum allowable number of iterations N without the update is the algorithm control parameter: its decrease potentially leads to enhancing the design quality, whereas diminishing N is advantageous for lowering the computational cost (the results of Table III have been obtained for N = 3). More details on Algorithm 2 can be found in [55].
- Algorithm 3: the expedited version of the reference TR algorithm involving sensitivity updating formulas, also exclusively based on high-fidelity EM simulations. In this procedure, for the directions that are sufficiently well aligned with the most recent design relocation, the Jacobian matrix is updated with a rank-one Broyden formula (BF) rather than through FD. The following alignment factors are defined

$$\gamma_k^{(i)} = \left| \boldsymbol{h}^{(i)T} \boldsymbol{e}^{(k)} \right| / \left\| \boldsymbol{h}^{(i)} \right\|, \quad k = 1, \ldots, n, \qquad (12)$$

where $\boldsymbol{e}^{(k)}$ corresponds to the standard basis vectors (i.e., $\boldsymbol{e}^{(k)}$ contains only zeros except for 1 on the k-th position), and $\boldsymbol{h}^{(i+1)} = \boldsymbol{x}^{(i+1)} - \boldsymbol{x}^{(i)}$. For a given parameter k, if $\gamma_k^{(i)}$ is larger than a user-defined threshold $\gamma_{\min}$, the appropriate Jacobian portion is updated with BF. The algorithm control parameter $0 \le \gamma_{\min} \le 1$ can be used to govern the trade-offs between the computational savings and the design quality. As $\gamma_{\min}$ gets higher, the condition for using BF gets more rigorous; hence, FD is performed more often and the design quality likely increases. For a more detailed account of Algorithm 3, see [23].

C. Results

Tables III through VI gather the numerical results obtained with the proposed and the benchmark algorithms. For illustration purposes, Fig. 7 shows the reflection characteristics at the selected initial and optimized designs of Antennas I through IV. Figure 8 shows the relationships between the model resolution and antenna reflection for Antennas III and IV, respectively. As mentioned before, the data provided in the tables is based on ten independent algorithm runs initiated from random starting points.

TABLE III NUMERICAL RESULTS FOR ANTENNA I

Algorithm	Performance figure				
	Cost[1]	Cost savings[2]	max|S_{11}|[3]	Δ max|S_{11}|[4]	Std max|S_{11}|[5]
Conventional TR search	97.6	–	–11.9	–	0.4
Accelerated TR search [58]	45.1	53.8	–11.1	0.8	1.0
Accelerated TR search [30]	53.0	46%	–10.7	1.2	2.7
Multi-fidelity (this work)	48.2	51%	–11.2	0.7	0.7

[1] Number of equivalent high-fidelity EM simulations averaged over 10 algorithm runs.
[2] Relative computational savings in percent w.r.t. the reference algorithm.
[3] Objective function value (max. in-band reflection in dB), averaged over 10 algorithm runs.
[4] Degradation of max|S_{11}| w.r.t. the TR algorithm in dB, averaged over 10 algorithm runs.
[5] Standard deviation of max|S_{11}| in dB across the set of 10 algorithm runs.

TABLE IV NUMERICAL RESULTS FOR ANTENNA II

Algorithm	Performance figure				
	Cost[1]	Cost savings[2]	max|S_{11}|[3]	Δ max|S_{11}|[4]	Std max|S_{11}|[5]
Conventional TR search	111.2	–	–14.9	–	0.6
Accelerated TR search [58]	58.3	48%	–13.7	1.2	1.3
Accelerated TR search [30]	75.9	32%	–14.3	0.6	1.0
Multi-fidelity (this work)	25.8	77%	–13.8	1.1	1.0

[1] Number of equivalent high-fidelity EM simulations averaged over 10 algorithm runs.
[2] Relative computational savings in percent w.r.t. the reference algorithm.
[3] Objective function value (max. in-band reflection in dB), averaged over 10 algorithm runs.
[4] Degradation of max|S_{11}| w.r.t. the TR algorithm in dB, averaged over 10 algorithm runs.
[5] Standard deviation of max|S_{11}| in dB across the set of 10 algorithm runs.

This article has been accepted for publication in a future issue of this journal, but has not been fully edited. Content may change prior to final publication. Citation information: DOI 10.1109/TAP.2021.3083742, IEEE Transactions on Antennas and Propagation

TABLE V NUMERICAL RESULTS FOR ANTENNA III

Algorithm	Performance figure				
	Cost[1]	Cost savings[2]	max|S_{11}|[3]	Δ max|S_{11}|[4]	Std max|S_{11}|[5]
Conventional TR search	111.0	–	–13.9	–	1.0
Accelerated TR search [55]	73.1	34%	–12.8	1.1	1.3
Accelerated TR search [23]	80.0	28%	–11.9	1.9	2.0
Multi-fidelity (this work)	42.3	62%	–11.3	2.6	1.0

[1] Number of equivalent high-fidelity EM simulations averaged over 10 algorithm runs.
[2] Relative computational savings in percent w.r.t. the reference algorithm.
[3] Objective function value (max. in-band reflection in dB), averaged over 10 algorithm runs.
[4] Degradation of max|S_{11}| w.r.t. the TR algorithm in dB, averaged over 10 algorithm runs.
[5] Standard deviation of max|S_{11}| in dB across the set of 10 algorithm runs.

TABLE VI NUMERICAL RESULTS FOR ANTENNA IV

Algorithm	Performance figure				
	Cost[1]	Cost savings[2]	max|S_{11}|[3]	Δ max|S_{11}|[4]	Std max|S_{11}|[5]
Conventional TR search	139.7	–	–17.6	–	1.2
Accelerated TR search [55]	91.2	34%	–16.3	1.3	2.5
Accelerated TR search [23]	89.2	36%	–15.1	2.5	2.6
Multi-fidelity (this work)	97.2	31%	–17.0	0.6	2.1

[1] Number of equivalent high-fidelity EM simulations averaged over 10 algorithm runs.
[2] Relative computational savings in percent w.r.t. the reference algorithm.
[3] Objective function value (max. in-band reflection in dB), averaged over 10 algorithm runs.
[4] Degradation of max|S_{11}| w.r.t. the TR algorithm in dB, averaged over 10 algorithm runs.
[5] Standard deviation of max|S_{11}| in dB across the set of 10 algorithm runs.

Shown are: the cost of the optimization process expressed in the (equivalent) number of high-fidelity antenna simulations, the cost savings with respect to the conventional TR algorithm, as well as the quality indicators. These include the average objective function value (here, the maximum in-band reflection), quality degradation with respect to the conventional algorithm, as well as the standard deviation of the objective function value as a repeatability of results metric. The latter is to be compared to that of the conventional algorithm for the reasons elaborated on in Section III.B. The optimization cost of the proposed multi-fidelity algorithm is computed by taking into account the time evaluation ratios of the low- and the high-fidelity models throughout the optimization run.

D. Discussion

The results presented in Section III.*C* allow us to draw some conclusions concerning the performance of the proposed multi-fidelity optimization algorithm in relation to the reference routines. These can be summarized as follows:

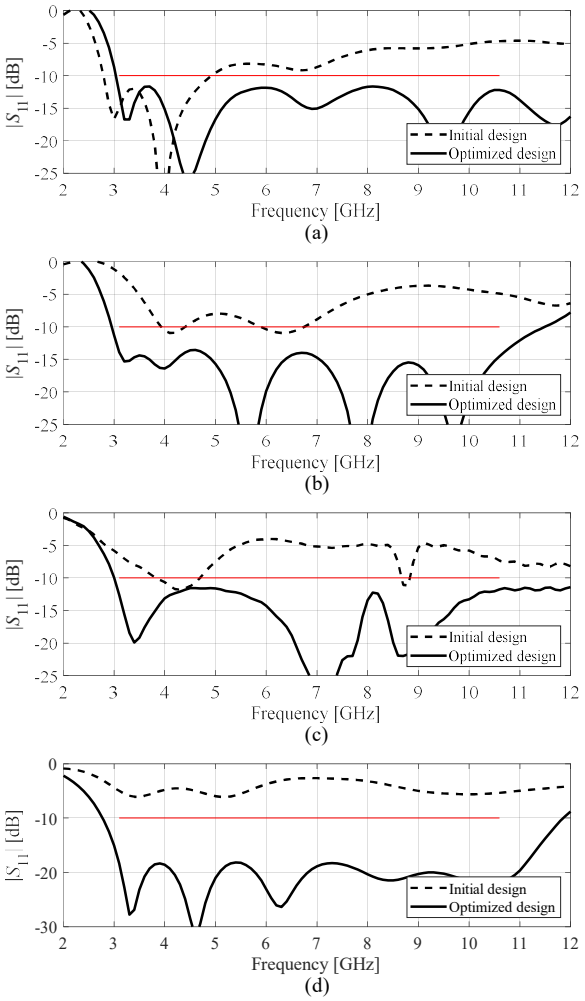

Fig. 7. Reflection responses for the representative runs of the proposed multi-fidelity algorithm: (a) Antenna I, (b) Antenna II, (c) Antenna III, (d) Antenna IV. Design specifications marked using the horizontal lines; (- - -) initial design, (—) optimized design. The provided plots are obtained at the high-fidelity level of resolution for the respective antenna structures.

- The proposed multi-fidelity algorithm offers considerable speedup with respect to the conventional TR procedure, which is from over 30 to almost 80 percent (over 55 percent on the average) across the considered antenna benchmark set;
- The computational efficiency of the proposed algorithm is either comparable (for Antennas I and IV), or significantly better (for Antennas II and III) than that of the accelerated versions [23] and [55]. These results are correlated with the evaluation time relationships for multi-fidelity EM models as presented in Table II and Fig. 6, where the time evaluation ratios between the high- and lowest-fidelity models are 3.6, 10.3, 5.8, and 2.6 for Antennas I through IV. This suggests that extending the range of discretization densities might have a positive effect on the computational efficiency. It should also be mentioned that L_{max} selected for all test cases does not really correspond to the high-fidelity model but it was treated as such in order to be consistent with the experimental data in the literature [23], [55]. Increasing L_{max} would lead to the improvement of the computational savings.

This article has been accepted for publication in a future issue of this journal, but has not been fully edited. Content may change prior to final publication. Citation information: DOI 10.1109/TAP.2021.3083742, IEEE Transactions on Antennas and Propagation

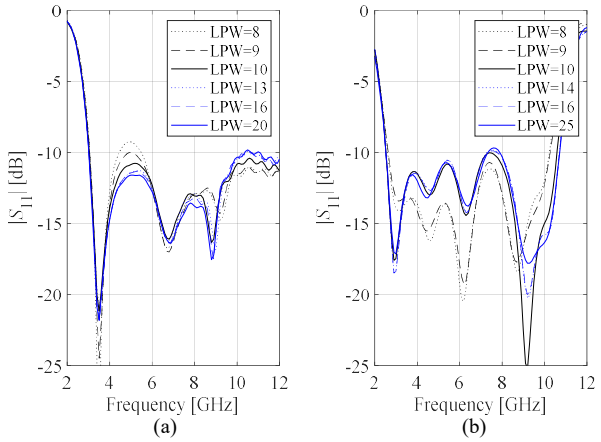

Fig. 8. The family of reflection responses corresponding to various discretization densities of the structure (controlled using the LPW parameter) for (a) Antenna III, and (b) Antenna IV.

- The proposed multi-fidelity algorithm leads to a certain degradation of the design quality as compared to the conventional TR procedure; however, this degradation is not significant, around 1dB in terms of the objective function value on the average. On the other hand, the repeatability of solutions measured using standard deviation is similar to that of the conventional algorithm.
- When comparing the design quality between the proposed algorithm and the two accelerated versions of [23] and [55], apart from Antenna III, it is comparable or in favor of the proposed approach, especially for Antenna IV. In terms of repeatability, the proposed algorithm exhibits the lowest standard deviation.

Overall, it can be concluded that the presented multi-fidelity algorithm ensures significant computational speedup while maintaining practically acceptable reliability. At the same time, it should be mentioned that the proposed approach employs full finite-differentiation-based sensitivity updates at each stage of the optimization process. Part of the future work will be to incorporate some of the acceleration mechanisms, similar to those of [23] and [55], which is likely to foster further improvements, especially in terms of the computational efficiency of the framework.

IV. Conclusion

The paper proposed a novel algorithm for accelerated trust-region gradient-based optimization of antenna input characteristics involving multi-fidelity EM-simulation models. Our methodology is based on a decision making procedure that permits a continuous adjustment of the model fidelity depending on the convergence status of the optimization process. At the initial stages, the lower-fidelity (and cheaper) simulations are employed with the computational model resolution gradually increasing towards the end of the process. The high-fidelity model is only used when close to convergence to secure reliability. The presented approach leads to significant computational savings of up to almost eighty percent, when compared to conventional trust-region approach. The fundamental contributor to these is the problem-specific knowledge extracted at a low cost from coarse-discretization antenna models. The aforementioned benefits have been demonstrated using a comprehensive test set of four broadband antennas optimized multiple times using random initial designs. At the same time, our algorithm ensures better design quality than the recently reported accelerated procedures with sparse sensitivity updates, while maintaining comparable or better computational efficiency. The proposed approach can be viewed as an alternative to standard local search techniques, offering a considerable reduction of the computational expenses by capitalizing on the efficient management of variable-fidelity models. Although the considered antenna examples are of rather low computational complexity (simulation times of a few minutes for the respective high-fidelity models), the percentage-wise savings are expected to be similar for more complex problems. This is because the latter only depend on the time-evaluation ratio between the lower-fidelity models and the high-fidelity one. These ratios are generally similar for the range of computational models, including the relatively complex ones.

The future work will be focused on further developments, in particular, the incorporation of the acceleration mechanisms in the form of restricted Jacobian matrix updates, which will likely lead to additional cost reduction. The relationships between the algorithm performance, EM model discretization levels, and the associated simulation times, will be investigated as well, in order to identify the best possible setups of the computational models and the algorithm control parameters.

Acknowledgment

The authors would like to thank Dassault Systemes, France, for making CST Microwave Studio available.

References

[1] J. Zeng and K. Luk, "Single-layered broadband magnetoelectric dipole antenna for new 5G application," *IEEE Ant. Wireless Prop. Lett.*, vol. 18, no. 5, pp. 911-915, 2019.

[2] M. Rokunuzzaman, A. Ahmed, T. C. Baum, and W. S. T. Rowe, "Compact 3-D antenna for medical diagnosis of the human head," *IEEE Trans. Ant. Prop.*, vol. 67, no. 8, pp. 5093-5103, 2019.

[3] I. A. Shah, M. Zada, and H. Yoo, "Design and analysis of a compact-sized multiband spiral-shaped implantable antenna for scalp implantable and leadless pacemaker systems," *IEEE Trans. Ant. Prop.*, vol. 67, no. 6, pp. 4230-4234, 2019.

[4] Y. Zheng, G. A. E. Vandenbosch, and S. Yan, "Low-profile broadband antenna with pattern diversity," *IEEE Ant. Wireless Prop. Lett.*, vol. 19, no. 7, pp. 1231-1235, 2020.

[5] X. Cai and K. Sarabandi, "Broadband omnidirectional circularly polarized antenna with asymmetric power divider," *IEEE Trans. Ant. Prop.*, vol. 68, no. 7, pp. 5171-5181, 2020.

[6] J. Nagar, R. J. Chaky, M. F. Pantoja, A. F. McKinley, and D. H. Werner, "Optimization of far-field radiation from impedance-loaded nanoloops accelerated by an exact analytical formulation," *IEEE Trans. Ant. Prop.*, vol. 67, no. 3, pp. 1448-1458, 2019.

[7] Y. Hu, Z. Qiu, B. Yang, S. Shi, and J. Yang, "Design of novel wideband circularly polarized antenna based on Vivaldi antenna structure," *IEEE Ant. Wireless Prop. Lett.*, vol. 14, pp. 1662-1665, 2015.

[8] S. J. Yang, Y. D. Kim, D. J. Yun, D. W. Yi, and N. H. Myung, "Antenna modeling using sparse infinitesimal dipoles based on recursive convex optimization," *IEEE Ant. Wireless Prop. Lett.*, vol. 17, no. 4, pp. 662-665, 2018.

[9] S. Koziel, S. Ogurtsov, W. Zieniutycz, and L. Sorokosz, "Expedited design of microstrip antenna subarrays using surrogate-based optimization," *IEEE Ant. Wireless Prop. Lett.*, vol. 13, pp. 635-638, 2014.

[10] M. Kovaleva, D. Bulger, B. A. Zeb, and K. P. Esselle, "Cross-entropy method for electromagnetic optimization with constraints and mixed variables," *IEEE Trans. Ant. Prop.*, vol. 65, no. 10, pp. 5532-5540, 2017.

[11] M. Ohira, A. Miura, M. Taromaru, and M. Ueba, "Efficient gain optimization techniques for azimuth beam/null steering of inverted-F multiport parasitic array radiator (MuPAR) antenna," *IEEE Trans. Ant. Prop.*, vol. 60, no. 3, pp. 1352-1361, 2012.

[12] J. Wang, X. S. Yang, and B. Z. Wang, "Efficient gradient-based optimization of pixel antenna with large-scale connections," *IET Microwaves Ant. Prop.*, vol. 12, no. 3, pp. 385-389, 2018.

[13] S. Koziel, "Computationally efficient multi-fidelity multi-grid design optimization of microwave structures," *Applied Comp. Electromagnetics Society J.*, vol. 25, no. 7, pp. 578-586, 2010.

[14] S. K. Goudos, K. Siakavara, and J. N. Sahalos, "Novel spiral antenna design using artificial bee colony optimization for UHF RFID applications," *IEEE Ant. Wireless Prop. Lett.*, vol. 13, pp. 528-531, 2014.

[15] A. A. Minasian and T. S. Bird, "Particle swarm optimization of microstrip antennas for wireless communication systems," *IEEE Trans. Ant. Prop.*, vol. 61, no. 12, pp. 6214-6217, 2013.

[16] Y. Rahmat-Samii, J. M. Kovitz, and H. Rajagopalan, "Nature-inspired optimization techniques in communication antenna designs," *Proc. IEEE*, vol. 100, no. 7, pp. 2132-2144, 2012.

[17] A. Darvish and A. Ebrahimzadeh, "Improved fruit-fly optimization algorithm and its applications in antenna arrays synthesis," *IEEE Trans. Ant. Prop.*, vol. 66, no. 4, pp. 1756-1766, 2018.

[18] A. Aldhafeeri and Y. Rahmat-Samii, "Brain storm optimization for electromagnetic applications: continuous and discrete," *IEEE Trans. Ant. Prop.*, vol. 67, no. 4, pp. 2710-2722, 2019.

[19] A. Kouassi, N. Nguyen-Trong, T. Kaufmann, S. Lalléchère, P. Bonnet, and C. Fumeaux, "Reliability-aware optimization of a wideband antenna," *IEEE Trans. Ant. Prop.*, vol. 64, no. 2, pp. 450-460, 2016.

[20] J. Du and C. Roblin, "Statistical Modeling of Disturbed Antennas Based on the Polynomial Chaos Expansion," *IEEE Ant. Wireless Prop. Lett.*, vol. 16, pp. 1843-1846, 2017.

[21] A. Pietrenko-Dabrowska, S. Koziel, and M. Al-Hasan, „Expedited yield optimization of narrow- and multi-band antennas using performance-driven surrogates," *IEEE Access*, pp. 143104-143113, 2020.

[22] E. Hassan, D. Noreland, R. Augustine, E. Wadbro, and M. Berggren, "Topology optimization of planar antennas for wideband near-field coupling," *IEEE Trans. Ant. Prop.*, vol. 63, no. 9, pp. 4208-4213, 2015.

[23] S. Koziel and A. Pietrenko-Dabrowska, "Expedited optimization of antenna input characteristics with adaptive Broyden updates," Eng. Comp., vol. 37, no. 3, 2019.

[24] J. C. Cervantes-González, J. E. Rayas-Sánchez, C. A. López, J. R. Camacho-Pérez, Z. Brito-Brito, and J. L. Chávez-Hurtado, "Space mapping optimization of handset antennas considering EM effects of mobile phone components and human body," *Int. J. RF Microwave CAE*, vol. 26, no. 2, pp. 121-128, 2016.

[25] J. A. Easum, J. Nagar, P. L. Werner, and D. H. Werner, "Efficient multi-objective antenna optimization with tolerance analysis through the use of surrogate models," *IEEE Trans. Ant. Prop.*, vol. 66, no. 12, pp. 6706-6715, 2018.

[26] S. Koziel and S. Ogurtsov, *Antenna design by simulation-driven optimization. Surrogate-based approach*, Springer, New York, 2014.

[27] J. W. Bandler, Q. S. Cheng, S. A. Dakroury, A. S. Mohamed, M. H. Bakr, K. Madsen, and J. Sondergaard, "Space mapping: the state of the art," *IEEE Trans. Microwave Theory Tech.*, vol. 52, no. 1, pp. 337-361, 2004.

[28] F. Feng, J. Zhang, W. Zhang, Z. Zhao, J. Jin, and Q. J. Zhang, "Coarse- and fine-mesh space mapping for EM optimization incorporating mesh deformation," *IEEE Microwave Wireless Comp. Lett.*, vol. 29, no. 8, pp. 510-512, 2019.

[29] S. Koziel and S. D. Unnsteinsson, "Expedited design closure of antennas by means of trust-region-based adaptive response scaling," *IEEE Antennas Wireless Prop. Lett.*, vol. 17, no. 6, pp. 1099-1103, 2018.

[30] S. Koziel, "Fast simulation-driven antenna design using response-feature surrogates," *Int. J. RF & Microwave CAE*, vol. 25, no. 5, pp. 394-402, 2015.

[31] C. Zhang, F. Feng, V. Gongal-Reddy, Q. J. Zhang, and J. W. Bandler, "Cognition-driven formulation of space mapping for equal-ripple optimization of microwave filters," *IEEE Trans. Microwave Theory Techn.*, vol. 63, no. 7, pp. 2154-2165, 2015.

[32] A. K. S. O. Hassan, A. S. Etman, and E.A. Soliman, "Optimization of a novel nano antenna with two radiation modes using kriging surrogate models," *IEEE Photonic J.*, vol. 10, no. 4, art. no. 4800807, 2018.

[33] P. Barmuta, F. Ferranti, G. P. Gibiino, A. Lewandowski, and D. M. M. P. Schreurs, "Compact behavioral models of nonlinear active devices using response surface methodology," *IEEE Trans. Microwave Theory and Tech.,* vol. 63, no. 1, pp. 56-64, 2015.

[34] J. P. Jacobs, "Characterization by Gaussian processes of finite substrate size effects on gain patterns of microstrip antennas," *IET Microwaves Ant. Prop.*, vol. 10, no. 11, pp. 1189-1195, 2016.

[35] A. Petrocchi, A. Kaintura, G. Avolio, D. Spina, T. Dhaene, A. Raffo, and D. M. P. P. Schreurs, "Measurement uncertainty propagation in transistor model parameters via polynomial chaos expansion," *IEEE Microwave Wireless Comp. Lett.*, vol. 27, no. 6, pp. 572-574, 2017.

[36] A. Rawat, R. N. Yadav, and S. C. Shrivastava, "Neural network applications in smart antenna arrays: a review," *AEU – Int. J. Elec. Comm.*, vol. 66, no. 11, pp. 903-912, 2012.

[37] J. Cai, J. King, C. Yu, J. Liu, and L. Sun, "Support vector regression-based behavioral modeling technique for RF power transistors," *IEEE Microwave and Wireless Comp. Lett.,* vol. 28, no. 5, pp. 428-430, 2018.

[38] J. A. Easum, J. Nagar, and D. H. Werner, "Multi-objective surrogate-assisted optimization applied to patch antenna design," *Int. Symp. Ant. Prop.*, pp. 339-340, San Diego, USA, 2017.

[39] A. M. Alzahed, S. M. Mikki, and Y. M. M. Antar, "Nonlinear mutual coupling compensation operator design using a novel electromagnetic machine learning paradigm," *IEEE Ant. Wireless Prop. Lett.*, vol. 18, no. 5, pp. 861-865, 2019.

[40] J. Tak, A. Kantemur, Y. Sharma, and H. Xin, "A 3-D-printed W-band slotted waveguide array antenna optimized using machine learning," *IEEE Ant. Wireless Prop. Lett.*, vol. 17, no. 11, pp. 2008-2012, 2018.

[41] H. M. Torun and M. Swaminathan, "High-dimensional global optimization method for high-frequency electronic design," *IEEE Trans. Microwave Theory Techn.*, vol. 67, no. 6, pp. 2128-2142, 2019.

[42] S. Koziel and A. T. Sigurdsson, "Triangulation-based constrained surrogate modeling of antennas," *IEEE Trans. Ant. Prop.*, vol. 66, no. 8, pp. 4170-4179, 2018.

[43] A. Toktas, D. Ustun, and M. Tekbas, "Multi-objective design of multi-layer radar absorber using surrogate-based optimization," *IEEE Trans. Microw. Theory Techn*., vol. 67, no. 8, pp. 3318-3329, 2019.

[44] Z. Lv, L. Wang, Z. Han, J. Zhao, and W. Wang, "Surrogate-assisted particle swarm optimization algorithm with Pareto active learning for expensive multi-objective optimization," *IEEE/CAA J. Automatica Sinica*, vol. 6, no. 3, pp. 838-849, 2019.

[45] D. K. Lim, D. K. Woo, H. K. Yeo, S. Y. Jung, J. S. Ro, and H. K. Jung, "A novel surrogate-assisted multi-objective optimization algorithm for an electromagnetic machine design," *IEEE Trans. Magn*., vol. 51, no. 3, paper 8200804, 2015.

[46] G. Oliveri, A. Gelmini, A. Polo, N. Anselmi, and A. Massa, "System-by-Design Multiscale Synthesis of Task-Oriented Reflectarrays," *IEEE Trans. Ant. Prop.*, vol. 68, no. 4, pp. 2867-2882, 2020.

[47] G. Oliveri, M. Salucci, N. Anselmi, and A. Massa, "Multiscale system-by-design synthesis of printed WAIMs for waveguide array enhancement," *IEEE J. Multiscale Multiphysics Comp. Techn.*, vol. 2, pp. 84-96, 2017.

[48] A. Massa, G. Oliveri, P. Rocca, and F. Viani, "System-by-design: A new paradigm for handling design complexity, *European Conf. Ant. Propag (EuCAP)*, The Hague, Netherlands, 2014, pp. 1180-1183.

[49] E. T. Bekele, G. Oliveri, E. Martini, S. Maci, and A. Massa, "A material-by-design strategy for the design and optimization of multisurface-metamaterial polarizers," *European Conf. Ant. Propag (EuCAP)*, The Hague, Netherlands, 2014, pp. 1965-1968.

[50] G. Oliveri, E. T. Bekele, M. Salucci, and A. Massa, "Transformation electromagnetics miniaturization of sectoral and conical metamaterial-enhanced horn antennas," *IEEE Trans. Ant. Prop.*, vol. 64, no. 4, pp. 1508-1513, 2016.

[51] C. Cui, Y. Jiao, and L. Zhang, „Synthesis of some low sidelobe linear arrays using hybrid differential evolution algorithm integrated with

convex programming," *IEEE Ant. Wireless Prop. Lett.*, vol. 16, pp. 2444-2448, 2017.

[52] M. Pazokian, N. Komjani, and M. Karimipour, „Broadband RCS reduction of microstrip antenna using coding frequency selective surface," *IEEE Ant. Wireless Prop. Lett.*, vol. 17, no. 8, pp. 1382-1385, 2018.

[53] S. Koziel and L. Leifsson, *Simulation-driven design by knowledge-based response correction techniques*, Springer, New York, 2016.

[54] S. Koziel and S. Ogurtsov, "Model management for cost-efficient surrogate-based optimization of antennas using variable-fidelity electromagnetic simulations," *IET Microwaves Ant. Prop.*, vol. 6, no. 15, pp. 1643-1650, 2012.

[55] S. Koziel and A. Pietrenko-Dabrowska, "Reduced-cost electromagnetic-driven optimization of antenna structures by means of trust-region gradient-search with sparse Jacobian updates," *IET Microwaves Ant. Prop.*, vol. 13, no. 10, pp. 1646-1652, 2019.

[56] S. Koziel and A. Pietrenko-Dabrowska, "Variable-fidelity simulation models and sparse gradient updates for cost-efficient optimization of compact antenna input characteristics," *Sensors*, vol. 19, no. 8, 2019.

[57] S. Koziel, S. D. Unnsteinsson, and A. Bekasiewicz "Low-fidelity model considerations for simulation-based optimization of miniaturized wideband antennas," *IET Microwaves, Ant. Prop.*, vol. 12, no. 10, pp. 1613-1619, 2018.

[58] C. Zhang, X. Fu, X. Chen, S. Peng, and X. Min, "Synthesis of uniformly excited sparse rectangular planar array for sidelobe suppression using multi-objective optimization algorithm," *J. Eng.*, vol. 2019, no. 19, pp. 6278-6281, 2019.

[59] R. T. Marler and J. S. Arora, "The weighted sum method for multi-objective optimization: new insights," *Structural Multidisc. Opt.*, vol. 41, pp. 853-862, 2010.

[60] U. Ullah, S. Koziel, and I. B. Mabrouk, "Rapid re-design and bandwidth/size trade-offs for compact wideband circular polarization antennas using inverse surrogates and fast EM-based parameter tuning," *IEEE Trans. Ant. Prop.*, vol. 68, no. 1, pp. 81-89, 2019.

[61] A. R. Conn, N. I. M. Gould, and P. L. Toint, *Trust Region Methods*, MPS-SIAM Series on Optimization, 2000.

[62] Y. Su, J. Li, Z. Fan, and R. Chen, „Shaping optimization of double reflector antenna based on manifold mapping," *Int. Applied Comp. Electromagnetics Soc. Symp. (ACES)*, Suzhou, China, pp. 1-2, 2017.

[63] B. Liu, S. Koziel, and N. Ali, "SADEA-II: a generalized method for efficient global optimization of antenna design," *J. Comp. Design Eng.*, vol. 4, no. 2, pp. 86-97, 2017.

[64] S. Koziel, A. Bekasiewicz, I. Couckuyt, and T. Dhaene, "Efficient multi-objective simulation-driven antenna design using co-kriging," *IEEE Trans. Antennas Prop.*, vol. 62, no. 11, pp. 5900-5905, 2014.

[65] S. Koziel and A. Bekasiewicz, "Low-cost multi-objective optimization of antennas using Pareto front exploration and response features," *Int. Symp. Antennas Prop.*, Fajardo, Puerto Rico, 2016.

[66] M. G. N. Alsath and M. Kanagasabai, "Compact UWB monopole antenna for automotive communications," *IEEE Trans. Ant. Prop.*, vol. 63, no. 9, pp. 4204-4208, 2015.

[67] M. A. Haq and S. Koziel, "Simulation-based optimization for rigorous assessment of ground plane modifications in compact UWB antenna design," *Int. J. RF Microwave CAE*, vol. 28, no. 4, e21204, 2018.

[68] D. R. Suryawanshi and B. A. Singh, "A compact UWB rectangular slotted monopole antenna", *IEEE Int. Conf. Control*, *Instrumentation, Comm. Comp. Tech.* (ICCICCT), pp. 1130-1136, 2014.

SLAWOMIR KOZIEL received the M.Sc. and Ph.D. degrees in electronic engineering from Gdansk University of Technology, Poland, in 1995 and 2000, respectively. He also received the M.Sc. degrees in theoretical physics and in mathematics, in 2000 and 2002, respectively, as well as the PhD in mathematics in 2003, from the University of Gdansk, Poland. He is currently a Professor with the Department of Engineering, Reykjavik University, Iceland. His research interests include CAD and modeling of microwave and antenna structures, simulation-driven design, surrogate-based optimization, space mapping, circuit theory, analog signal processing, evolutionary computation and numerical analysis.

ANNA PIETRENKO-DABROWSKA received the M.Sc. and Ph.D. degrees in electronic engineering from Gdansk University of Technology, Poland, in 1998 and 2007, respectively. Currently, she is an Associate Professor with Gdansk University of Technology, Poland. Her research interests include simulation-driven design, design optimization, control theory, modeling of microwave and antenna structures, numerical analysis.